Monthly Notices
of the
ROYAL ASTRONOMICAL SOCIETY

MNRAS **479,** 1800–1806 (2018)
Advance Access publication 2018 May 8

doi:10.1093/mnras/sty1196

An X-ray expansion and proper motion study of the Magellanic Cloud Supernova Remnant J0509–6731 with the *Chandra* X-ray observatory

Quentin Roper,[1]★ Miroslav Filipovic,[1] Glenn E. Allen,[2] Hidetoshi Sano,[3,4] Laurence Park,[1] Thomas G. Pannuti,[5] Manami Sasaki,[6] Frank Haberl,[7] Patrick J. Kavanagh,[8] Yumiko Yamane,[4] Satoshi Yoshiike,[4] Kosuke Fujii,[9] Yasuo Fukui[3,4] and Ivo R. Seitenzahl[10,11,12]

[1]*Western Sydney University, Locked Bag 1797, Penrith South DC, NSW 1797, Australia*
[2]*Kavli Institute for Astrophysics and Space Research, Massachusetts Institute of Technology, 77 Massachusetts Avenue, NE80-6025, Cambridge, MA 02139, USA*
[3]*Institute for Advanced Research, Nagoya University, Furo-cho, Chikusa-ku, Nagoya 464-8601, Japan*
[4]*Department of Physics, Nagoya University, Furo-cho, Chikusa-ku, Nagoya 464-8601, Japan*
[5]*Space Science Center, Department of Earth and Space Science, Morehead State University, 235 Martindale Drive, Morehead, KY 40351, USA*
[6]*Dr. Karl Remeis-Sternwarte, Erlangen Centre for Astroparticle Physics, Friedrich-Alexander-University Erlangen-Nurnberg, Sternwartstraße 7, Bamberg D-96049, Germany*
[7]*Max-Planck-Institut für extraterrestrische Physik, Giessenbachstr, Garching D-85748, Germany*
[8]*School of Cosmic Physics, Dublin Institute for Advanced Studies, 31 Fitzwilliam Place, Dublin 2, Ireland*
[9]*Department of Astronomy, School of Science, The University of Tokyo, 7-3-1 Hongo, Bunkyo-ku, Tokyo 133-0033, Japan*
[10]*School of Physical, Environmental and Mathematical Sciences, University of New South Wales, Australian Defense Force Academy, Canberra, ACT 2600, Australia*
[11]*Research School of Astronomy and Astrophysics, Australian National University, Canberra, Australia, 0200*
[12]*ARC Centre of Excellence for All-sky Astrophysics (CAASTRO)*

Accepted 2018 April 20. Received 2018 April 13; in original form 2017 June 5

ABSTRACT

Using archival *Chandra* data consisting of a total of 78.46 ksec over two epochs 7 yr apart, we have measured the expansion of the young (∼400 yr old) Type Ia Large Magellanic Cloud supernova remnant (SNR) J0509–6731. In addition, we use radial brightness profile matching to detect proper-motion expansion of this SNR, and estimate a speed of $7500 \pm 1700\,\mathrm{km\,s^{-1}}$. This is one of the only proper motion studies of extragalactic SNRs expansion that is able to derive an expansion velocity, and one of only two such studies of an extragalactic SNR to yield positive results in the X-rays. We find that this expansion velocity is consistent with an optical expansion study on this object. In addition, we examine the medium in which the SNR is expanding by examining the CO and neutral HI gas using radio data obtained from Mopra, the Australia Telescope Compact Array, and Parkes radio telescopes. We also briefly compare this result with a recent radio survey, and find that our results predict a radio spectral index α of -0.67 ± 0.07. This value is consistent with high-frequency radio observations of MCSNR J0509–6731.

Key words: supernovae:individual: SNR J0509-6731 – ISM: evolution – ISM:supernova remnants.

1 INTRODUCTION

Supernova remnants (SNRs) play a vital role in the physical evolution and chemical enrichment of the interstellar medium (ISM). Their precursors, supernovae (SNe), are believed to occur through two main scenarios: The first being core collapse events, which are the explosions of massive stars ($M \gtrsim 8\,\mathrm{M}_\odot$) and release large quantities of α-elements into the ISM. Secondly, thermonuclear SN (Type Ia) progenitors are less massive and are believed to be the resulting detonation of carbon–oxygen white dwarfs (WDs) that have reached the Chandrasekhar limit (∼1.4 $\mathrm{M}_\odot$). This may be the result of a single degenerate system, where a WD in a binary system will accrete matter from a companion star, or a double degenerate (DD) system, in which two WDs merge (thus exceeding the mass limit) and explode as an SN. The study of Type Ia SNe is not only

★ E-mail: Q.Roper@westernsydney.edu.au

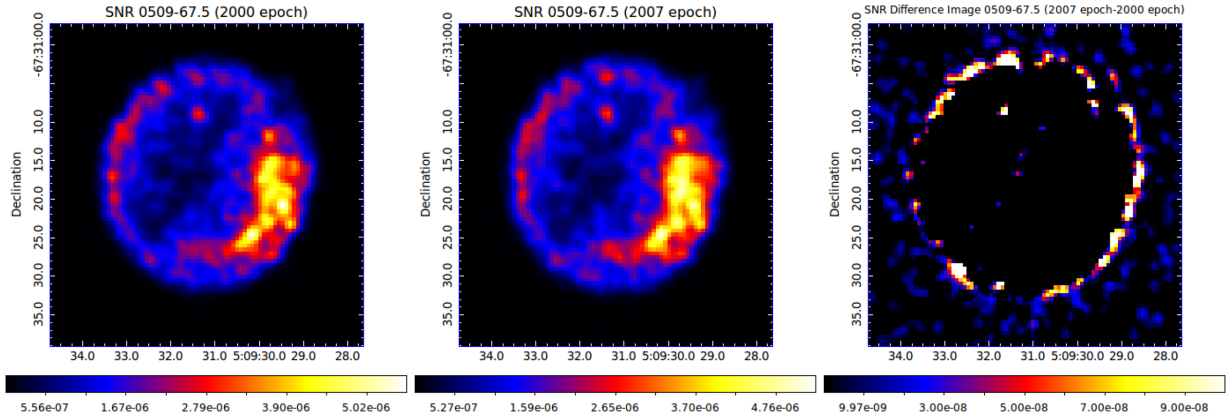

Figure 1. Left: The exposure and PSF-corrected 2000 epoch X-ray data of an SNR 0509–67.5. Centre: The exposure and PSF-corrected 2007 epoch X-ray data of an SNR 0509–67.5. Right: The difference image between the 2007 epoch and the 2000 epoch X-ray data. Notice the difference results in a nearly complete shell, indicating observable uniform expansion. The colour bar is in units of photons s^{-1} keV^{-1} cm^{-2}, smoothed over a Gaussian kernel with 2- pixel width. An enclosed counts fraction of 90 per cent was used in order to produce the PSF map. An energy range from 0.5–8.0 keV was used to produce this map, using 2.3 keV as a reference energy.

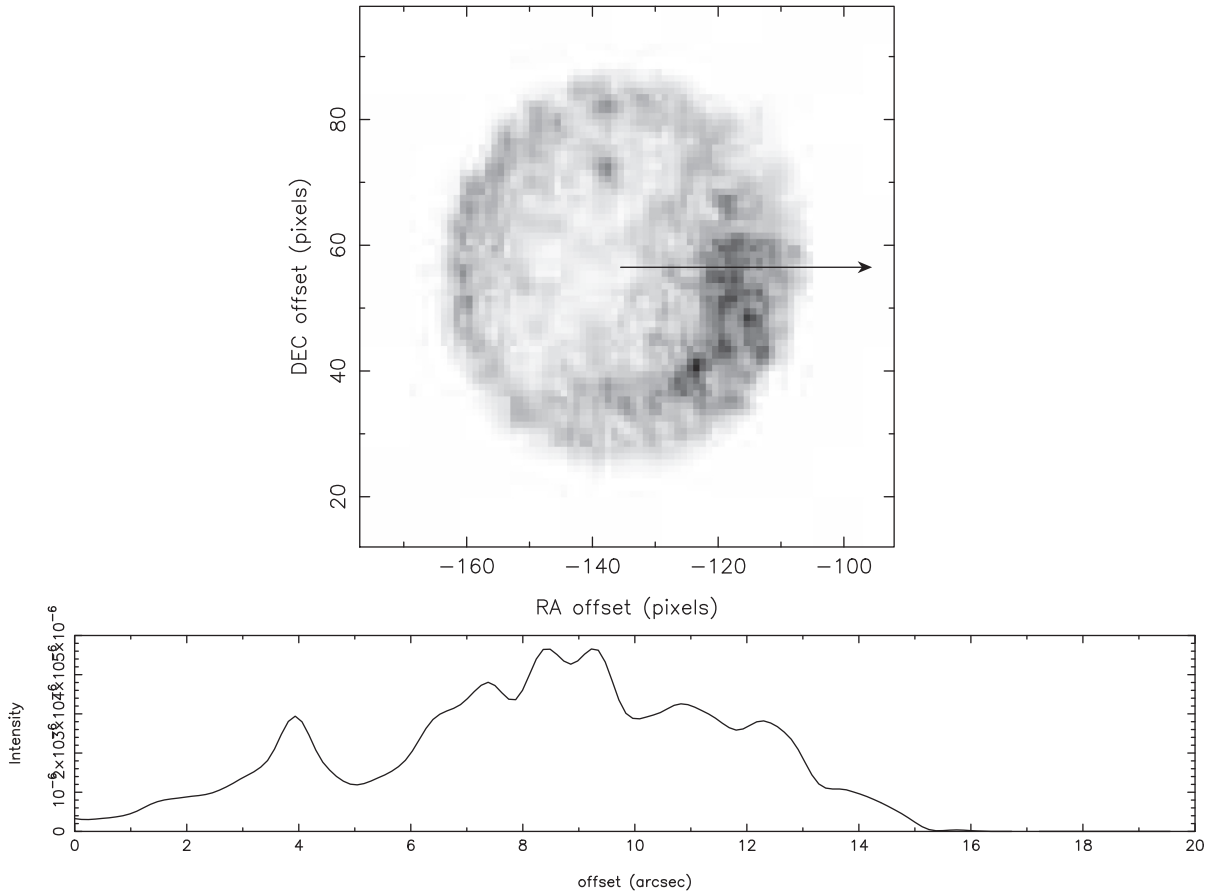

Figure 2. A visualization of the method described in the text – the top panel is the 2000 epoch X-ray data with a radial ray traced from the centre of the remnant outward, and the bottom panel is the surface brightness profile along that ray.

important due to their use as 'standard candles' in measuring cosmological distances, but also to ascertain the exact nature of the progenitor system.

Estimating the expansion velocity of an SNR given its age, size, and the density of the ambient ISM can constrain the explosion energy of the initial SN event by applying the Sedov–Taylor similarity solution (Sedov 1959). Accurate estimates of these quantities can provide important constraints to SNR evolution models, e.g. Cox (1972) and Badenes et al. (2006). In addition, SNRs are thought to be a major source of cosmic rays (Baade & Zwicky 1934; Gunn & Ostriker 1969). Understanding how the expansion velocity of SNRs evolves overtime can yield information on how cosmic rays

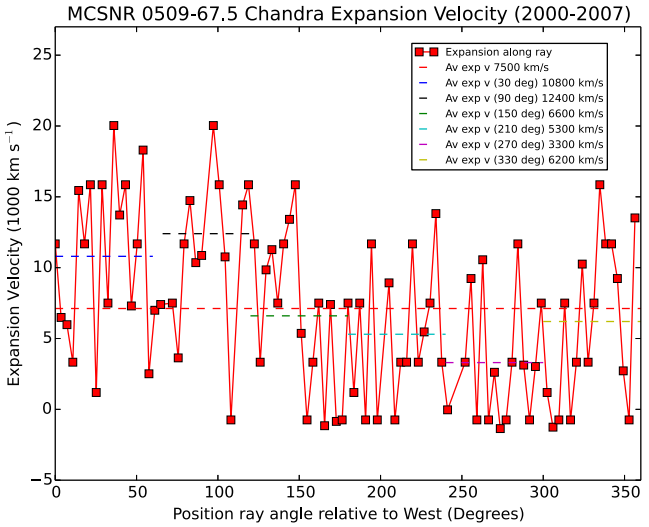

Figure 3. A graph of the expansion versus position angle of the ray along which the expansion is measured (solid line) as well as the average value across all position angles measured (red-dashed line). The average expansion value is 0.22 arcsec that corresponds to an expansion velocity of 7500 km s^{-1}. Also, overlaid on the plot is directional expansion velocities centred at position angles starting at 30° up to 330° at regular intervals.

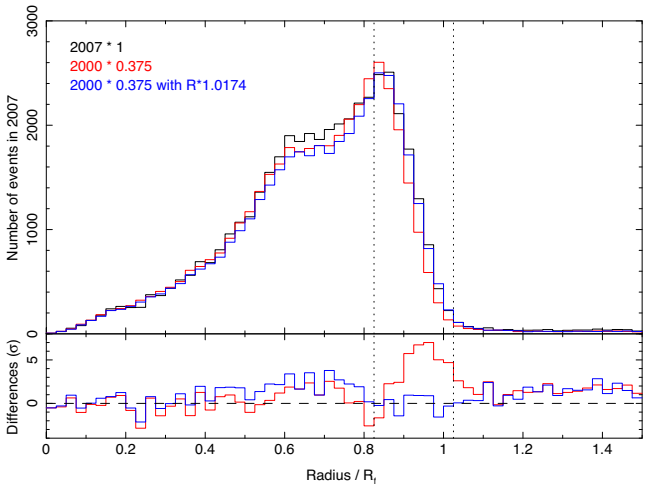

Figure 4. Profile modelling of the average counts profile of an SNR 0509–67.5. The red curve is the average X-ray counts profile of the 2000 epoch data, multiplied by a factor for the purpose of comparison to the 2007 epoch data. The black curve is the average X-ray counts profile of the 2007 epoch data. The green curve is the rescaled 2000 epoch data whose radius has been scaled by a factor of 1.02. The agreement between the green and black profile curves implies ∼1.74 per cent increase in radius between the two epochs that is in reasonably good agreement with our result.

are produced. Also a new diagnostic, the surface brightness index, which can be computed from theory and compared to *Chandra*, *Hubble Space Telescope* (*HST*), and radio observations, can be used to demonstrate that a DD progenitor can explain the decades-long flux density rise and size increase of the youngest Type Ia SNRs (Chakraborti, Childs & Soderberg 2016).

Young Type Ia SNRs in the Small Magellanic Cloud (SMC) and Large Magellanic Cloud (LMC) form an ideal sample to utilize the surface brightness index and thus understand the progenitor systems of those SNRs (Roper et al. 2015; Maggi et al. 2016; Bozzetto et al.

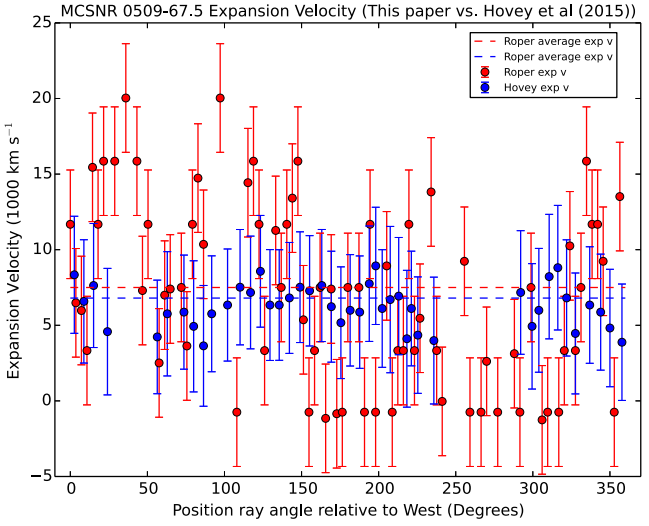

Figure 5. A comparison between the expansion versus position angle relative to due west. In the red is the expansion from the X-ray, and in the blue is the optical expansion reported by Hovey et al. (2015). The dashed lines represent the average expansion velocity as seen by Hovey et al. (2015) in blue and this paper (red).

2017). SNRs in the MCs are located outside the Galactic Plane that minimizes the interference from foreground Galactic dust, gas, and stars. Their position towards the South Ecliptic Pole – one of the coldest areas of the radio sky – minimizes the influence of Galactic foreground radiation. The proximity of the LMC (∼50 kpc; Pietrzyński et al. 2013) and SMC (∼60 kpc; Hilditch, Howarth & Harries 2005) from us is quite far, so we are able to assume all objects that lie within are at approximately the same distance. At the same time, these sources are close enough that we can resolve extended spatial structure in these objects. Thus, the SNRs in the Magellanic Clouds constitute a particularly useful sample for the study of an SNR and related phenomena.

An SNR 0509–67.5 is the second youngest SNR in the LMC, with an angular size of ∼31arcsec. From light echo studies, its age is estimated to be 400 ± 120 yr (Rest et al. 2005). Badenes et al. (2008) utilized *Chandra* and *XMM–Newton* data to perform X-ray imaging spectroscopy studies, and through hydrodynamic delayed detonation modelling and SNR evolution models found that an SNR 0509–67.5 was likely the result of Type Ia SN explosion. In addition, an *HST* H α study of an SNR 0509–67.5 with a baseline of 1 yr carried out by Hovey, Hughes & Eriksen (2015) estimated its expansion velocity to be 6500 ± 200 km s^{-1}; the authors associate this expansion velocity with the forward shock velocity. In addition to estimating the cosmic ray acceleration rate in this SNR, they use this expansion velocity to argue that 0509–67.5 is somewhat younger than the age estimate placed on it by Rest et al. (2005), estimating the age as 310^{+40}_{-30} yr old. Furthermore, they are able to derive an expansion parameter of $0.57^{+0.08}_{-0.05}$ that led them to conclude that J0509-6731 is still in an ejecta-dominated phase of its evolution. The goal of this study is to use archival X-ray data taken by multiple separate observations of the *Chandra X-ray Telescope* to estimate the proper-motion expansion of an SNR 0509–67.5.

2 OBSERVATIONS AND METHODOLOGY

We utilize two archival *Chandra* ACIS observations of an SNR 0509–67.5, one observed in 2000 May (OBSID 776, 50 ks) and

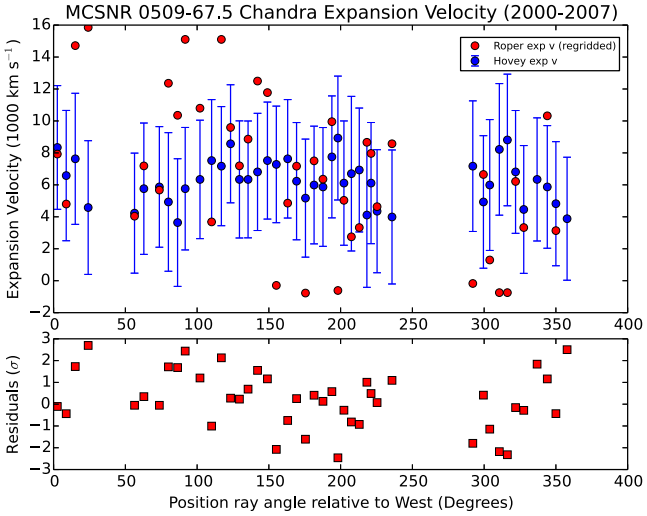

Figure 6. Results of the χ^2 comparison to Hovey et al. (2015), with the data from that study in blue (with error bars that indicate the combined error between the data presented in this paper and that of Hovey et al. 2015), and the results from this paper are in red. The lower plot shows the residuals from the χ^2 in terms of the errors in the data from this paper and that of Hovey et al. (2015) added in quadrature.

another in 2007 May (OBSID 8554, 30 ks). These two observations were also used in the Badenes et al. (2008) study. Both observations have an SNR 0509–67.5 at their nominal aim points (Fig. 1). We use these two observations with a temporal baseline of 7 yr in order to perform proper-motion detection of the expansion of an SNR 0509–67.5 and estimate its expansion velocity. In addition, the right-hand panel of Fig. 1 shows a simple pixel-by-pixel subtraction image, which was then smoothed with a Gaussian kernal of 2 pixels, and suggests that this remnant has expanded to an observable degree in the 7.02 yr difference between the two observations.

First, we used standard CIAO 4.8 data-reduction techniques to produce flux-corrected images and maps of the point spread function (PSF) across both images, with *FLUXIMAGE* and *MKPSFMAP*. We used an enclosed counts fraction of 90 per cent in order to produce the PSF map. The ACIS PSF is energy dependent; an energy range from 0.5–8.0 keV was used to produce this map, approximating 2.3 keV as a reference energy. This results in the images in the left-hand and centre panel of Fig. 1.

To perform this proper-motion detection, we examine the flux intensity profile of the SNR in both the 2000 epoch and the 2007 epoch data. We limit the number of position angles along which the expansion is measured by the angular size of the remnant. To accomplish this, relative astrometry corrections were applied between the 2000 epoch and the 2007 epoch data using CIAO 4.8. Specifically, we used *wavdetect*, utilizing the PSF maps produced in the previous step to detect point sources in common between the two images and then use *wcs_match* and *wcs_update* to calculate and apply the astrometric correction. Four point sources were found in common between the two observations. The plate scale and rotation between the two observations were held fixed and the only degrees of freedom allowed to vary in the match were translation in the right ascension and declination. The total relative astrometric correction applied was 0.55 ± 0.10 pixels, or 0.27 ± 0.05 arcsec. The centre of the remnant was chosen to be at RA(J2000) = $05^{\rm h}09^{\rm m}31.19^{\rm s}$ and Dec(J2000) = –67°31′17.″0.

The MIRIAD (Sault, Teuben & Wright 1995) task *CGSLICE*[1] is designed to produce the brightness profile along a line segment in the image in regular intervals, interpolating using nearest neighbour interpolation at points where the segment does not fall exactly at the centre of a pixel in the image. After the astrometric correction was applied, we used *cgslice* to measure the radial brightness profile of an SNR 0509–67.5 in both the 2000 epoch and 2007 epoch data to compute the change in radius of the remnant between the two epochs. In case a profile does not lie exactly along a set of pixels, the brightness profile is produced by a nearest neighbour interpolation of surrounding pixels. We produce 100 separate brightness profiles evenly spaced in a position angle for both the 2000 epoch data and the 2007 epoch data. For reference, Fig. 2 visualizes the brightness profile of a position angle of 0° that was chosen by convention, to be due west. Each subsequent position angle is 3.6° different from the previous one. This set of angles was chosen so that the edge of the SNR along a given angle was on a distinct pixel, so that the measured edge of the SNR along each position angle was independent of the edge measured along every other position angle. It should be noted that, near the centre of the remnant, adjacent brightness profiles are not independent as they have contribution from the same pixel. However, we only consider the portion of the brightness profiles near the edge of the remnants, where adjacent brightness profiles fall on separate pixels in this study.

To measure the degree of expansion along each position angle ray, we artificially expand the outer 7 arcsec of the brightness profile along the position angle ray in the 2000 epoch observation, interpolate the resulting shifted 2000 epoch brightness profile on to the corresponding brightness profile in the 2007 epoch observation. The expansion parameter was adjusted so that the χ^2 residuals between the 2007 epoch brightness profile and the shifted 2000 epoch brightness profile were minimized. In Hovey et al. (2015), this corresponds to equation (1) of that paper in subsection 3.1.1, given here, and modified to correspond to our data.

$$\chi^2 = \sum_{i=1}^{N} \frac{(R_{i,2007} - a_i R_{i,2000})^2}{\sigma_{i,2007}^2 + \langle a \rangle^2 \sigma_{i,2000}^2} \quad (1)$$

In equation (1), $R_{i,\,200X}$ is the radial brightness profile measurements of the two epochs, a_i is the expansion parameter of best fit, $\sigma_{i,\,200X}$ is the uncertainties in the brightness profile values, estimated as the local noise level. The term $\langle a \rangle$ denotes the average expansion parameter across the entire remnant.

The average expansion we measure between the two epochs has an uncertainty σ given by

$$\sigma = \sqrt{\frac{\theta^2 + 3w^2}{3n}}, \quad (2)$$

where $w = 0.492$ arcsec is the on-axis *Chandra* ACIS instrument resolution, n is the number of position angle rays along which we measure the expansion, and θ is the standard deviation of the expansion measurements. Using this, we were able to measure the average expansion of the SNR with a resolution 0.05 arcsecis better than the natural ACIS resolution of 0.492 arcsec (see Fig. 3). We constrain the number of position angles measured by the size of the remnant (∼31arcsec) such that each radial measurement should be on a different pixel. This restriction forces each position angle ray to be an independent measurement of the expansion. For illustrative purposes, Fig. 4 contains the average brightness profile curves of an SNR 0509–67.5 for the 2000 epoch and the 2007 epoch observation.

[1] www.atnf.csiro.au/computing/software/miriad/doc/cgslice.html

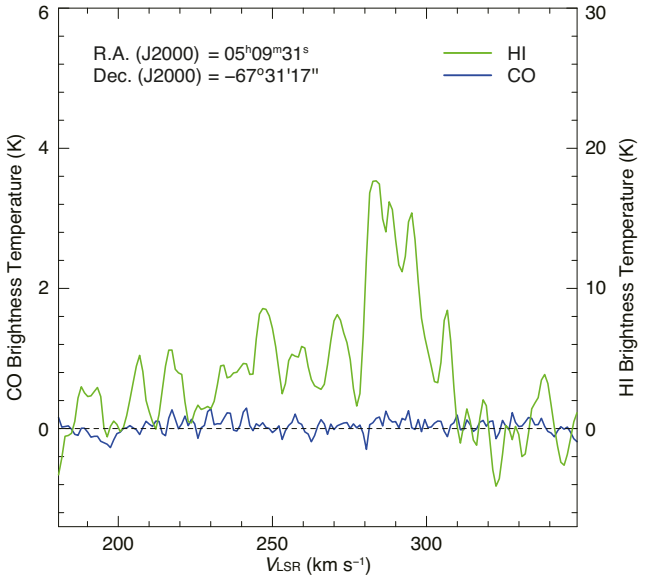

Figure 7. The results of the MOPS gas survey in the direction of an SNR 0509–67.5, with the CO gas content in blue, and the HI gas content in green. There is no significant amount of CO gas, indicating a rarefied medium, but the HI profile has a bump at a velocity range of ∼280–300 km s^{-1}, due to the disc component of the LMC.

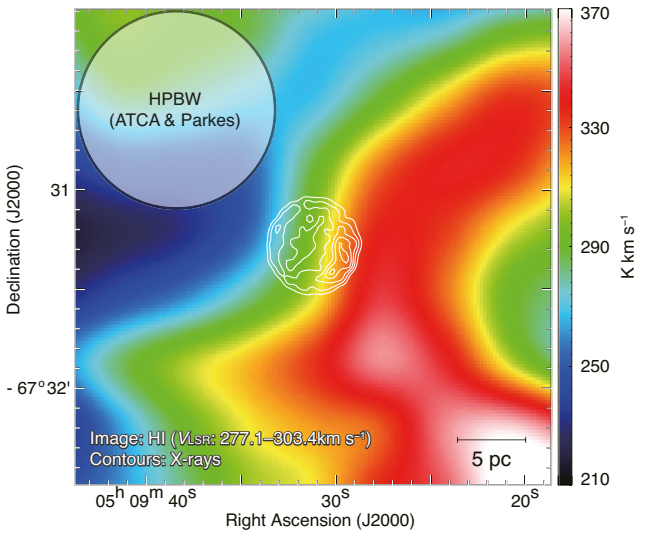

Figure 8. The neutral HI density in the vicinity of SNR 0509–67.5. The colour bar indicates the intensity of neutral HI gas along the line of sight of the SNR, with white X-ray contours overlaid on to the image. There is no indication of dense clouds near the remnant, indicating a rarefied ambient medium. There does appear to be a smooth gradient westward.

2.1 CO and hydrogen data

We also performed ^{12}CO(J = 1–0) observations using the Mopra 22-m radio telescope from 2014 May to 2014 October. We used the on-the-fly mapping mode with Nyquist sampling, and the observed area was 2 arcmin× 2 arcmin. The typical system temperature T_{sys} was 700–1100 K in the single-side band. The back end system, the Mopra Spectrometer (MOPS), provides 4096 channel bands (137.5 MHz), corresponding to a velocity resolution of ∼0.088 km s^{-1} and a velocity coverage of ∼360 km s^{-1}. The absolute intensity was calibrated by observing Orion–KL [RA(J2000) = $5^h35^m38.6^s$, Dec(J2000) = −5°22′30″; Ladd et al. 2005]. We also convolved the data with a Gaussian kernel, and final beam size was 45 arcsec. Finally, we combined the CO data cube with the Magellanic Mopra Assessment DR1 archival data (Wong et al. 2011) using the T_{sys} weighting method. The final noise fluctuation was 0.17 K at a velocity resolution of 0.53 km s^{-1}. We also used the archival Australia Telescope Compact Array and Parkes HI data set published by Kim et al. (2003). The angular resolution was ∼1 arcmin. The typical noise fluctuation was ∼2.4 Kat a velocity resolution of 1.649 km s^{-1}.

3 RESULTS

We found that an SNR 0509–67.5 radially expanded significantly by an average of 0.22 arcsec ± 0.05 arcsec (about 1.5 per cent over the 7.01 yr) between 2000 May and 2007 May that yields an expansion velocity v_{ex} of 7500 ± 1700 km s^{-1}. This fit is relatively good with a reduced χ^2 of 89.1/76. There were some rays along which an acceptable fit solution could not be obtained. There were three rays that have a spike of noise near the remnant edge in one epoch, but not the other. It may be that these anomalous sources are true X-ray transients or some other effect. In addition, there were some rays along which the fit converged to a solution with reduced $\chi^2 > 10.0$, which were disregarded in the final results. It is unclear why, in these cases, there does not appear to be a good fit to the 2007 epoch data. Finally, we ignored any results that implied an absolute value expansion velocity of $|v_{ex}| \geq 20\,000$ km s^{-1}. Including the data we ignored, we had a significantly worse-fit result (χ^2_r = 381.2/100) with a somewhat higher expansion velocity v_{ex} = (10 500 ± 2000) km s^{-1}. Furthermore, we compare the average X-ray counts profile. The average radial profile of the 2007 epoch data is very well described by the 2000 epoch data scaled by ∼1.7 per cent (Fig. 4).

We plot the expansion velocity versus position angle in Fig. 3. In this figure, we have adopted the convention that 0° is due west in the image. Additionally, overplotted on to this figure are the average expansion velocities in different directions at 60° intervals, starting at 30° up to a 330° maximum. There does appear to be some spatial variance to the expansion velocity, however it should be noted that these directional expansion velocities have much larger errors (∼4000 km s^{-1}) than the average expansion velocity, so these results are not statistically significant.

In order to more systematically compare our results to that of Hovey et al. (2015), we have graphed their expansion velocity versus position angle in Fig. 5. In addition, we have performed a χ^2 test using Hovey et al. (2015) data to model our own data. We interpolate our expansion data on to that of Hovey et al. (2015), and perform a simple χ^2 test using their results as a model for our data. This yields a reduced χ^2 of 77.9/44 ≈ 1.77. These results can be seen in Fig. 6. This value is relatively high and indicates formally that there is some statistical difference between the two data sets. This means that direct comparison between the two data sets with respect to directional expansion should be taken as suggestive rather than specifically indicative. However, while the reduced χ^2 is somewhat high, the lack of correlation in the residuals implies that our data are in relatively good agreement with that of Hovey et al. (2015).

3.1 The environment of interstellar molecular and atomic gases

Fig. 7 shows the ^{12}CO(J = 1−0) and HI line profiles towards an SNR 0509–67.5. There is no CO emission with a significance of 3σ or

higher. On the other hand, the HI profile has a bump at a velocity range of ∼280–300 km s^{-1}. Fig. 8 shows the integrated intensity map of H I superposed on the X-ray contours. Towards the south-west, there is a HI intensity gradient increasing from east, and the most prominent features, with H I intensities above 300 K km s^{-1}, lie in the south-west region. Unfortunately, we could not reveal a spatial correspondence between the HI and X-ray shell, due to a poor spatial resolution of H I data (∼15 pc at the LMC). The proton column density around the SNR is estimated to be ∼4–6 × 10^{20} cm^{-2} using the optically thin assumption (e.g. Dickey & Lockman 1990).

4 DISCUSSION AND CONCLUSIONS

Other than an SNR 1987A, this is one of the only two extragalactic SNR for which proper-motion expansion has been detected in the X-ray, with the other being SNR 0102–72.3 (Hughes, Rakowski & Decourchelle 2000). Its expansion has been detected to a significance level of ∼4.4. While this does not quite meet the 5σ standard that is well adopted in astrophysics, it is statistically significant to a p-value of ∼1.1 × 10^{-4}. This result could be improved by a similarly deep *Chandra* observation. At the estimated expansion velocity of 7500 km s^{-1}, an additional X-ray observation of this object taken at the time of publication or later would yield a total average angular expansion of $\gtrsim$0.50 arcsec thatis larger than the native *Chandra* ACIS resolution of 0.492 arcsec.

As stated in Section 3, there appears to be some spatial dependence in the expansion velocity. At its maximum, the average expansion velocity is in excess of 12 000 km s^{-1}, but the error on this quantity is large, about 5000 km s^{-1}. Although statistically not very significant, it should be noted that the expansion velocity is slowest in the south-west that is spatially coincident with a limb-brightened feature in the X-rays.

However, even if we measure the same forward shock velocity as in Hovey et al. (2015), this is still anomalously high for a Type Ia SNR. For comparison, Kepler's SNR, a Type Ia SNR at 410 yr, which is very similar to the light echo measurements of the age of an SNR 0509–67.5, is estimated to be travelling at ∼1700 km s^{-1} (Katsuda et al. 2015). More interestingly, this large expansion velocity could be indicative of a Type Ia DD scenario as Chakraborti et al. (2016) similarly argued for the youngest Galactic SNR G1.9+0.3 (also Type Ia). However, it should be noted that Kepler's slower expansion speed is due, at least in part, to a significant interaction with a denser than an average ISM (Katsuda et al. 2015).However, a more apt comparison might be Galactic SN 1006, which is somewhat older than the estimated age of an SNR 0509–67.5, and SN 1006 that has a simlar low-density ISM. In addition, optical proper-motion expansion speed estimates, as observations indicate, an expansion velocity as high as 5000 km s^{-1} (Katsuda et al. 2013). This is well consistent with our results of a younger SNR 0509–67.5 with an expansion velocity of ∼7500 km s^{-1}.

It is considered that a dynamical interaction between the SNR shock waves and an ISM affects the evolution of SNRs through the distortion of the shell morphology, if the ISM is dense enough. In an SNR 0509–67.5, we claim that a negligible amount of interstellar gas is interacting with the SNR. According to the recent studies of young Galactic/Magellanic SNRs interacting with the ISM, typical proton column density of HI was estimated to be ∼4–5 × 10^{21} cm^{-2} (e.g. Fukui et al. 2012; Sano et al. 2016, 2017), which is ten times higher than that of SNR 0509–67.5. In addition, no dense molecular clouds were detected towards the SNR (see Fig. 8). It is therefore likely that the shock of an SNR 0509–67.5 was not significantly decreased by the interaction with a dense molecular/atomic gas that is consistent with the high shock speed observed by the X-ray brightness profile study. In any case, further radio observations using ALMA and ATCA should be needed to reveal the interstellar environment at a sub-pc scale. Fig. 8 shows a gradient of ambient ISM density towards the west, rwhich is oughly consistent with Fig. 3, that is indicative of a slower expansion speed towards the west of the remnant,

In Bozzetto et al. (2017), the authors examine cosmic ray acceleration losses in shell-type SNRs in the LMC based on previous work by Bell, Schure & Reville (2011). They examine deviation from $\gamma = 2$ power law predicted by simple second-order Fermi scattering. They modelled the young LMC SNR population with a logarithmic relation between the expansion velocity of young SNRs and their associated radio spectral index (eq. 25 of that paper). A derived expansion velocity of 7500 ± 1700 km s^{-1} implies a radio spectral index $\alpha = -0.67 \pm 0.07$.[2] This is consistent with radio estimates of the radio spectral index of this SNR, measured at −0.71 ± 0.02 (Bozzetto et al. 2014, 2017). The results in this paper are consistent with the idea that radio spectral index is generally a good predictor of the expansion velocity of young SNRs, although it should be noted that an SNR 0509 is expanding into an abnormally underdense ISM, and so this result should be taken with a grain of salt.

ACKNOWLEDGEMENTS

The authors would like to acknowledge the efforts of the Chandra X-ray Center for maintaining the CIAO software as well as maintaining and curating the *Chandra Data Archive*. MS acknowledges support by the Deutsche Forschungsgemeinschaft through the research grant SA 2131/4-1 and the Heisenberg professor grant SA 2131/5-1.

REFERENCES

Baade W., Zwicky F., 1934, Contrib. Mount Wilson Obs., 3, 79
Badenes C., Hughes J. P., Cassam-Chenaï G., Bravo E., 2008, ApJ, 680, 1149
Badenes C., Borkowski K. J., Hughes J. P., Hwang U., Bravo E., 2006, ApJ, 645, 1373
Bell A. R., Schure K. M., Reville B., 2011, MNRAS, 418, 1208
Bozzetto L. M. et al., 2017, ApJS, 230, 2
Bozzetto L. M., Filipović M. D., Urošević D., Kothes R., Crawford E. J., 2014, MNRAS, 440, 3220
Chakraborti S., Childs F., Soderberg A., 2016, ApJ, 819, 37
Cox D. P., 1972, ApJ, 178, 159
Dickey J. M., Lockman F. J., 1990, ARA&A, 28, 215
Fukui Y. et al., 2012, ApJ, 746, 82
Gunn J. E., Ostriker J. P., 1969, Phys. Rev. Lett., 22, 728
Hilditch R. W., Howarth I. D., Harries T. J., 2005, MNRAS, 357, 304
Hovey L., Hughes J. P., Eriksen K., 2015, ApJ, 809, 119
Hughes J. P., Rakowski C. E., Decourchelle A., 2000, ApJ, 543, L61
Katsuda S. et al., 2015, ApJ, 808, 49
Katsuda S., Long K. S., Petre R., Reynolds S. P., Williams B. J., Winkler P. F., 2013, ApJ, 763, 85
Kim S., Staveley-Smith L., Dopita M. A., Sault R. J., Freeman K. C., Lee Y., Chu Y.-H., 2003, ApJS, 148, 473
Ladd N., Purcell C., Wong T., Robertson S., 2005, PASA, 22, 62
Maggi P. et al., 2016, A&A, 585, A162
Pietrzyński G. et al., 2013, Nature, 495, 76
Rest A. et al., 2005, Nature, 438, 1132

[2]This follows the convention that $S_\nu \propto \nu^\alpha$.

Roper Q., McEntaffer R. L., DeRoo C., Filipovic M., Wong G. F., Crawford E. J., 2015, ApJ, 803, 106
Sano H. et al., 2016, J. High Energy Astrophys., 15, 1
Sano H. et al., 2017, ApJ, 843, 61
Sault R. J., Teuben P. J., Wright M. C. H., 1995, in Shaw R. A., Payne H. E., Hayes J. J. E., eds, ASP Conf. Ser. Vol. 77, Astronomical Data Analysis Software and Systems IV. Astron. Soc. Pac., San Francisco, p. 433
Sedov L. I., 1959, Similarity and Dimensional Methods in Mechanics. Academic Press, New York
Wong T. et al., 2011, ApJS, 197, 16

This paper has been typeset from a TEX/LATEX file prepared by the author.